Asian Pub. Corp.

www.asianpubs.org

ARTICLE

Preparation, Structural and Optical Properties of SnO_2 Thin Films Prepared by Sol-Gel Method

Sariya D. Al-Algawi[1], Rashed T. Rasheed[2,✉], Hadeel S. Mansor[3] and Eman A. Jassem[2]

Asian Journal of Materials Chemistry

Volume: 2 Year: 2017
Issue: 1 Month: January-March
pp: 30–34
DOI: https://doi.org/10.14233/ajmc.2017.AJMC-P33

Received: 20 December 2016
Accepted: 10 January 2017
Published: 24 February 2017

ABSTRACT

Tin dioxide thin films were prepared by sol-gel dip coating technique using $SnCl_2 \cdot 2H_2O$ and ammonium hydroxide solution. The obtained thin film slides have been annealed at different temperature (200, 400 and 600 °C) in air at constant time (90 min). Structure and surface morphology of SnO_2 thin films were investigated and characterized by X-ray diffraction, atomic force microscope, scanning electron microscope, UV/visible and FTIR measurements. The optical properties of SnO_2 thin film were studied, such as transmittance, extinction coefficient, absorption coefficient and optical energy gap. The X-ray diffraction indicates a decreasing in crystaline size with increasing of doping concentration. The optical energy band gap was increased with the annealing temperature in range of (3.6 to 3.9) eV.

KEYWORDS

SnO_2 thin film, X-ray diffraction, Morphology, Energy gap.

INTRODUCTION

In recent years, semiconductor metal oxide have received considerable attention because of their possible application in gas sensor, solar cells, photochemical and photoconductive device, liquid crystal display, gas discharge display, lithium-ion batteries, *etc.* [1-3]. Tin dioxide (SnO_2) is an n-type semiconductor which has a strong gas sensing properties with wide energy band gap (3.6-3.8 eV) [4-6]. It is one of the extensively used metal oxide semiconductor due to its chemical and mechanical stabilities, pertaining to its unique electronic, magnetic and optical properties [4]. Oxide semiconductors such as SnO_2, In_2O_3, ZnO and WO_3 are representative the most used n-type semiconductor in gas sensing device materials for detecting trace concentrations of gases such as H_2S, H_2, CO, CH_4, C_3H_8, C_2H_5OH, CH_3COCH_3 and NO_2 [7].

The properties of SnO_2 that control its potential applications depend on the different phases of its fabrication history, synthesis routes and methods. In addition to the chemistry of the material, the morphological properties of powders influence their physical and chemical properties. In a sol-gel process the precursor solution is transformed into an inorganic solid by (a) dispersion of colloidal particles in a liquid (sol) and (b)

Author affiliations:

[1]Applied Physics Division, School of Applied Sciences, University of Technology, Baghdad, Iraq
[2]Applied Chemistry Division, School of Applied Sciences, University of Technology, Baghdad, Iraq
[3]Material Science Division, School of Applied Sciences, University of Technology, Baghdad, Iraq

✉To whom correspondence to be addressed:

E-mail: r_awsy@yahoo.com

Available online at: http://ajmc.asianpubs.org

conversion of sol into rigid phase (gel) by hydrolysis and condensation reactions. For various applications, nanosized particle or large specific surface area is essential to high performance [8].

A variety of techniques have been used to prepare tin dioxide thin films. These include spray pyrolysis [9], chemical vapour deposition [10], thermal beam evaporation [11], pulse laser deposition [12] and sputtering techniques [13]. Among these techniques sol-gel dip coating technique has proved to be simple, reproducible and inexpensive, as well as this method lowers the processing temperature, better homogeneity, controlled stoichiometry, flexibility of forming dense monoliths, thin films, nanoparticles and suitable for large area applications [8]. However it is only for last two decades that considerable interest, both in scientific and industrial fields, has been generated due to the realization of the several advantages one gets as compared to some other techniques. Sol-gel dip coating formation is usually a low temperature process. It requires less energy consumption and causes less pollution too [14]. In this paper we presented the formation and properties of SnO_2 thin film nanoparticles using sol-gel route.

EXPERIMENTAL

The structure of tin dioxide thin films were examined by X-ray diffractometer (6000 Shimadzu) using CuK_α radiation with a wavelength, $\lambda = 1.54060$ Å. The infrared spectra of the prepared nanoparticales with KBr disc were recorded using: FTIR-8400S Shimadzu in the range of 4000-400 cm^{-1}. Electronic spectra were obtained by using of UV/VIS-1650 PC Shimadzu spectrophotometer at wavelength (200-1100) nm. Size and surface distribution of SnO_2 nanopar-ticles were measured using atomic force microscope (AFM), using a scanning probe microscopy (CSPM-5000) instrument.

Preparation of tin dioxide nanoparticles: The tin dioxide nanoparticles were prepared by the sol-gel method [15]. In a typical procedure, (2 g, 8.85 mmol) stannous chloride dihydrate ($SnCl_2{\cdot}2H_2O$) (99.8 %, Aldrich) was dissolved in (20 mL) absolute ethanol. The solution was stirred with a magnetic stirrer for 0.5 h in a beaker, the solution become colourless. Ammonium hydroxide was added dropwise (one drop in 0.5 min) to the solution until the final solution pH value of about 8. The mixture was filtered in a centrifuge, then washed with a small portion of deionized water (repeat step twice), SnO_2 gelatin solution is obtained.

In hydroxyl solution, $SnCl_2$ was surrounded by OH^- ions and Cl^- was replaced by OH^- ions. In this condition, the following mechanisms may be involved during reaction in air. After reaction, white precipitate powder of SnO_2 nanoparticles was formed. The general suggested reaction between stannous chloride dihydrated and ammonium hydroxide solution are:

1. $SnCl_2{\cdot}2H_2O + 2NH_4OH \rightarrow Sn(OH)_2 + 2NH_4Cl + 2H_2O$
2. $Sn(OH)_2 \rightarrow SnO + H_2O$
3. $SnO + 1/2O_2 \rightarrow SnO_2$

The overall equation is:

$$SnCl_2{\cdot}2H_2O + 2NH_4OH + 1/2O_2 \rightarrow SnO_2 + 2NH_4Cl + 3H_2O$$

Preparation of thin film slides: A quartz slide is used as substrate for deposition SnO_2. This process can be summarized in the following steps: (1) the quartz substrate was washed with distilled water and cleaning powder to remove any oil or dust that might be on the substrate surface. (2) the quartz slides are placed in a clean beaker containing HCl acid (for 5 min). (3) the quartz slides are then placed in a clean beaker containing ethanol (for 15 min). (4) finally put in ultrasonic bath with distilled water for 15 min then dry. Dissolved part of the SnO_2 gelatin solution in 15 mL of absolute ethanol and put on the heating plate magnetic stirrer at 40 °C for 90 min. Take clean quartz slide and immerse in SnO_2 solution for a minute and dried quartz slide repeat this process several times (7-9) in order to be a homogeneous layer on the slide.

RESULTS AND DISCUSSION

Characterization of SnO_2 nanoparticles: The XRD is employed for the identification and understanding the crystalline growth nature of tin dioxide nanoparticles prepared by sol gel method at different annealing temperatures (200, 400, 600) °C for 90 min in air. The annealing temperature plays an important role in determining the structure of SnO_2 nanoparticles, the X-ray diffraction patterns of SnO_2 nanoparticles show high diffraction peaks showing good crystallinity. The diffraction peaks agree with those given in JCPD data card of bulk tetragonal SnO_2 refections from (110), (101) and (211), it can be seen that all the annealed SnO_2 thin film nanoparticles are polycrystalline with a tetragonal structure. The diffraction pattern of SnO_2 as prepared at (200 °C) shows three different located peaks (110), (101) and (211) at (2θ = 25.89, 33.83 and 52.03°), respectively. When they annealed thin film to (400 °C) many different located peaks appears (110), (101), (211), (310), (112) and (321) at (2θ = 25.71, 33.94, 52.42, 63.02, 66.2 and 79.438°), respectively. When they annealed to (600 °C) four different located peak appears (110), (101), (200), (211), (220), (112), (202) and (321) at (2θ = 26.70, 33.991, 38.05, 51.90, 54.83, 65.96, 71.4, and 78.8°), respectively.

From Fig. 1(a-c), it can be seen that there is an increasing in intensity of (110) orientation, this may due to heat treatment that enhances the mobility of atoms in rearrangement processes inside the lattice. The heat energy that provided to the atoms could decrease the defect in the SnO_2 nanoparticles and improve quality. This leads to decreases in full width at half maximums (FWHM) of the reflection peaks which become narrower as the particle size increases (Fig. 1c), which is a general size-dependent phenomenon within nanoparticles.

Film morphology

Surface morphology atomic force macroscopic (AFM): The surface morphology of SnO_2 nanoparticles was analyzed using atomic force microscope. Fig. 2 shows a typical three dimensional AFM image of SnO_2 nanoparticles with annealing at 200, 400 and 600 °C. The average grain size found to be (76-98 nm). Atomic force macroscopic results show that the grain size increase by increasing temperature this is due to improving the crystalline of the particles. Fig. 2 as well as, shows the granularity cumulation distribution chart of SnO_2 with annealing.

Surface morphology by SEM: The SEM images of the SnO_2 thin film nanoparticles with 200, 400 and 600 °C annea-

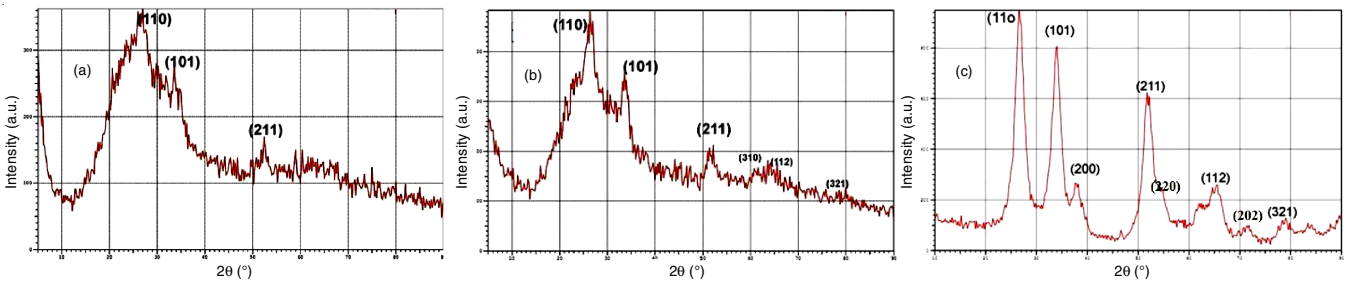

Fig. 1. XRD patterns of SnO_2 thin film nanoparticles at different annealing temperatures at (a) 200, (b) 400 and (c) 600 °C for 90 min

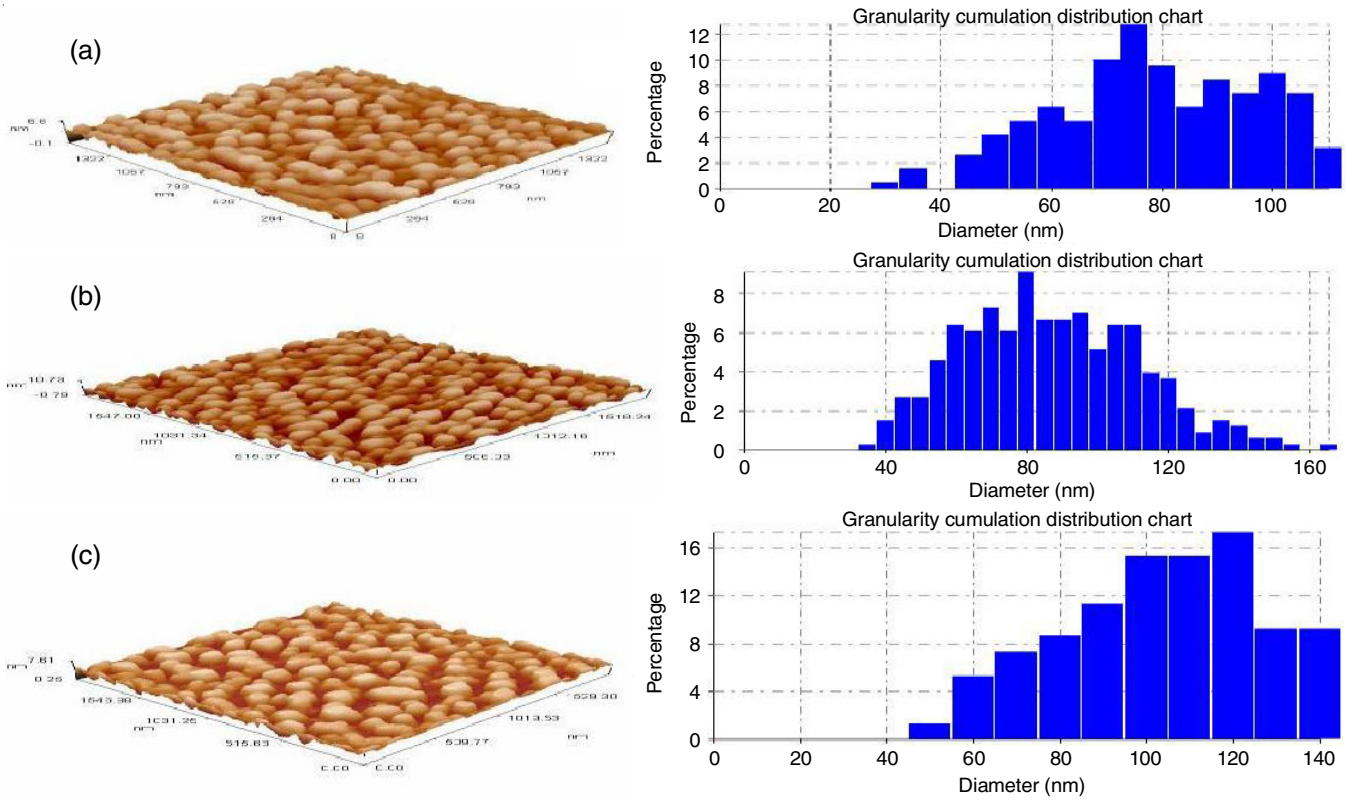

Fig. 2. Atomic force macroscopic image of SnO_2 nanoparticles with annealing at (a) 200, (b) 400 and (c) 600°C for 90 min

ling prepared by sol-gel methods have been shown in Fig. 3. As seen, nanoparticles have been grown as individual clusters with a few agglomerates over the surface. Particles sintered at lower temperature (as prepared and 200 °C), composed of large number of particulates with smaller sizes (Fig. 3a and 3b), respectively. On the other hand, particles sintered at higher temperature (400 and 600 °C), composed of less number of particulates with larger sizes (Fig. 3c and 3d), respectively, this was due to the growth and combination of small grains together after sintering process.

Effect of annealing temperature on FTIR: The FTIR spectra of SnO_2 nanopowders synthesized at the optimized preparation conditions and at different annealing temperatures are shown in Fig. 4. The most prominent absorption bands detected after thermal annealing are quite similar, with the main absorption bands (around 3420 cm^{-1}) due to water and low wave number bands (around 1630 cm^{-1}) attributed to O-H bending and the lowest bands (around 540 cm^{-1}) attributed to Sn-O band. These FTIR results corroborate those of thermal analysis [16].

Transmission, reflection and refraction index

Effect of annealing temperature: The effects of the annealing temperatures (200, 400 and 600 °C) for 90 min on SnO_2 thin films are shown in Figs. 5-7. It is found that the films have high transmission at long wavelengths reach to 90 % in the visible region and low reflection index. The optical transmission of SnO_2 thin films found to be increases with increasing annealing temperature. This is due to increasing of the orientation and this may due to heat treatment that enhances the mobility of atoms in rearrangement processes inside the lattice. The heat energy that provided to the atoms could decrease the defect in the SnO_2 nanoparticles and improve quality, the decreases in the UV-region (below 350 nm) is due to the fundamental absorption of light.

The optical reflection spectra and refractive index of SnO_2 thin films found to be decreasing with increasing annealing temperature, due to increasing of the orientation, and this may due to heat treatment that enhances the mobility of atoms in rearrangement processes inside the lattice.

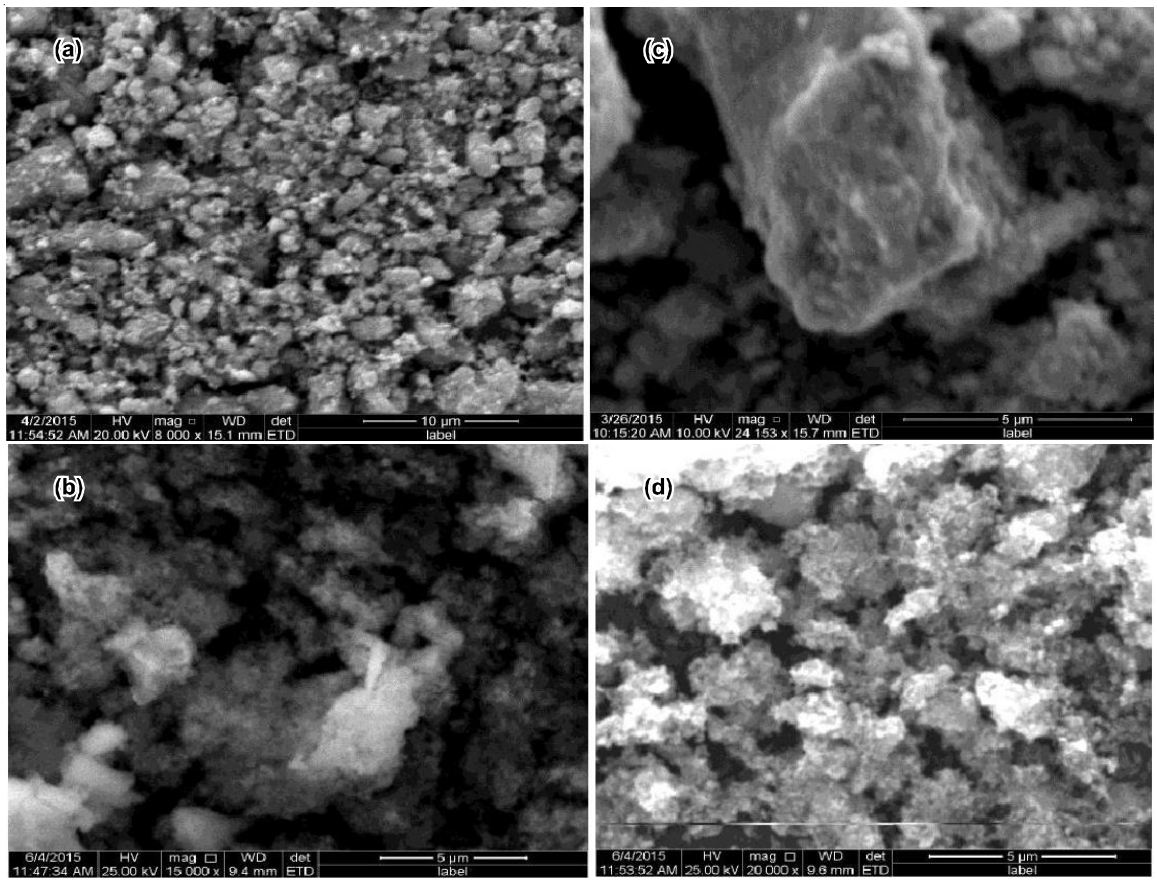

Fig. 3. SEM images of SnO_2 thin film nanoparticales: (a) asprepared, annealing at: (b) 200, (c) 400 and (d) 600 °C for 90 min

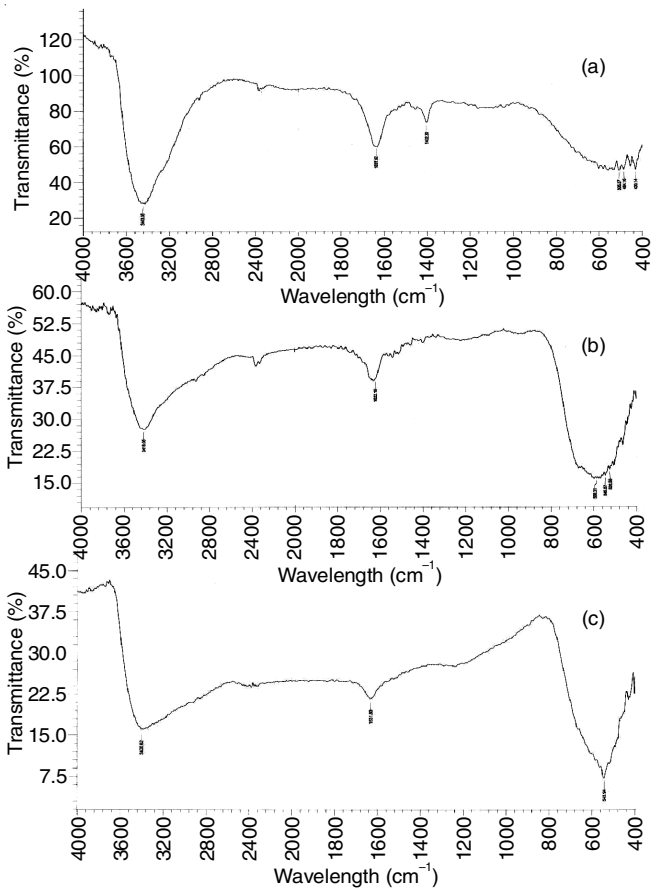

Fig. 4. FTIR spectra of SnO_2 thin film nanoparticles annealing at: (a) 200, (b) 400 and (c) 600 °C

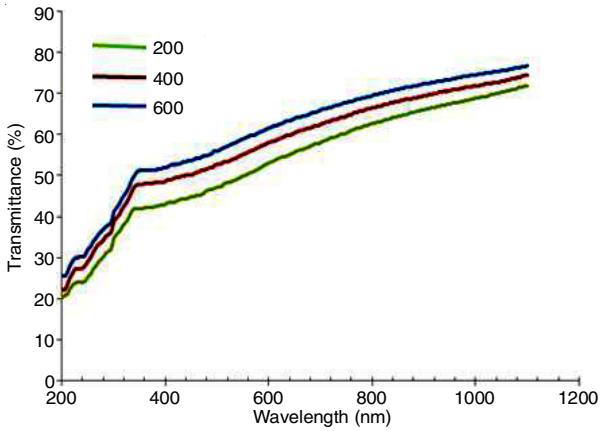

Fig. 5. UV-visible transmittance spectra of SnO_2 thin films at different annealing temperature (200, 400 and 600 °C)

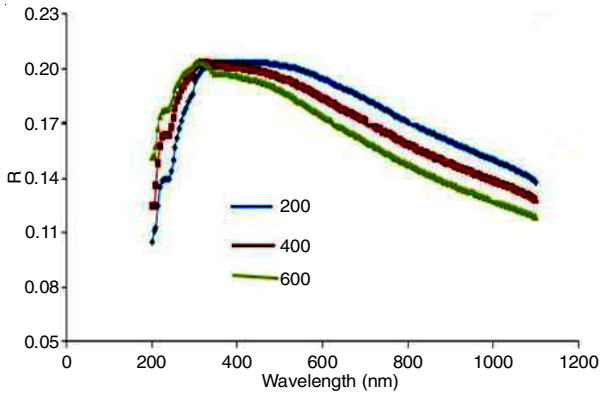

Fig. 6. UV-visible reflection spectra of SnO_2 thin films at different annealing temperature (200, 400 and 600 °C)

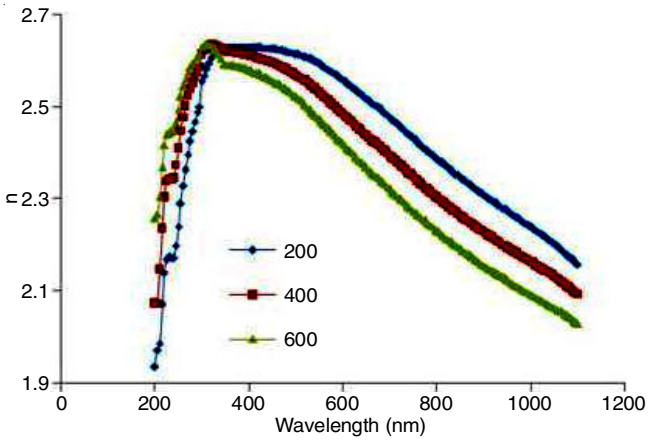

Fig. 7. UV-visible refractive index of SnO_2 thin films at different annealing temperature (200, 400 and 600 °C)

Conclusion

This study was focused on the influence of the annealing temperature (200, 400 and 600 °C) on the thin film of tin dioxide nanoparticles obtained by sol-gel process starting with stannous chloride dihydrate and ammonium hydroxide. The thin film annealing was characterized by XRD, AFM and SEM measurements. The XRD result reveal that SnO_2 nanoparticles have good crystallinity as they prepared and their crystallinity increase as they annealed to higher temperature. Energy band gap found to be increasing with the increasing in annealing temperature.

ACKNOWLEDGEMENTS

The authors are thankful for University of Technology laboratory and all laboratory staff who gave us assistance in the measurements.

REFERENCES

1. Y. Wang, X. Jiang and Y. Xia, *J. Am. Chem. Soc.*, **125**, 16176 (2003); https://doi.org/10.1021/ja037743f.
2. P.G. Harrison and M.J. Willett, *Nature*, **332**, 337 (1988); https://doi.org/10.1038/332337a0.
3. Y.S. He, J.C. Campbell, R.C. Murphy, M.F. Arendt and J.S. Swinnea, *J. Mater. Res.*, **8**, 3131 (1993); https://doi.org/10.1557/JMR.1993.3131.
4. G.E. Patil, D.D. Kajale, D.N. Chavan, N.K. Pawar, P.T. Ahire, S.D. Shinde, V.B. Gaikwad and G.H. Jain, *Bull. Mater. Sci.*, **34**, 1 (2011); https://doi.org/10.1007/s12034-011-0045-0.
5. L.C. Nehru, V. Swaminathan and C. Sanjeeviraja, *Am. J. Mater. Sci.*, **2**, 6 (2012); https://doi.org/10.5923/j.materials.20120202.02.
6. S. Gnanam and V. Rajendran, *Dig. J. Nanomater. Biostruct.*, **5**, 699 (2010).
7. N. Yamazoe, *Sens. Actuators B Chem.*, **108**, 2 (2005); https://doi.org/10.1016/j.snb.2004.12.075.
8. F. Gu, S.F. Wang, M.K. Lü, G.J. Zhou, D. Xu and D.R. Yuan, *J. Phys. Chem. B*, **108**, 8119 (2004); https://doi.org/10.1021/jp036741e.
9. K.S. Shamala, L.C.S. Murthy and K. Narasimha Rao, *Bull. Mater. Sci.*, **27**, 295 (2004); https://doi.org/10.1007/BF02708520.
10. G. Sanon, R. Rup and A. Mansingh, *Phys. Rev. B*, **44**, 5672 (1991); https://doi.org/10.1103/PhysRevB.44.5672.
11. D. Das and R. Banerjee, *Thin Solid Films*, **147**, 321 (1987); https://doi.org/10.1016/0040-6090(87)90028-9.
12. R. Dolbec, M.A. El Khakani, A.M. Serventi, M. Trudeau and R.G. Saint-Jacques, *Thin Solid Films*, **419**, 230 (2002); https://doi.org/10.1016/S0040-6090(02)00769-1.
13. R. Constantin and B. Miremad, *Surf. Coat. Technol.*, **120-121**, 728 (1999); https://doi.org/10.1016/S0257-8972(99)00366-7.
14. G. Zhang and M. Liu, *J. Mater. Sci.*, **34**, 3213 (1999); https://doi.org/10.1023/A:1004685907751.
15. M. Aziz, S. Saber Abbas and W.R. Wan Baharom, *Mater. Lett.*, **91**, 31 (2013); https://doi.org/10.1016/j.matlet.2012.09.079.
16. N. Nadaud, N. Lequeux, M. Nanot, J. Jové and T. Roisnel, *J. Solid State Chem.*, **135**, 140 (1998); https://doi.org/10.1006/jssc.1997.7613.
17. A. Solieman, *J. Sol-Gel Sci. Technol.*, **60**, 48 (2011); https://doi.org/10.1007/s10971-011-2549-x.